Impaired Anaplerosis Is a Major Contributor to Glycolysis Inhibitor Toxicity in Glioma

Sunada Khadka
The University of Texas MD Anderson Cancer Center
Kenisha Arthur
The University of Texas MD Anderson Cancer Center
Mykia Washington
The University of Texas MD Anderson Cancer Center
Yasaman Barekatain
The University of Texas MD Anderson Cancer Center
Jeff Ackroyd
The University of Texas MD Anderson Cancer Center
Eliot Behr
The University of Texas MD Anderson Cancer Center
Pornpa Suriyamongkol
The University of Texas MD Anderson Cancer Center
Yu-Hsi Lin
The University of Texas MD Anderson Cancer Center
Kaitlyn Crowley
The University of Texas MD Anderson Cancer Center
Cong-Dat Pham
The University of Texas MD Anderson Cancer Center
Dimitra K. Georgiou
The University of Texas MD Anderson Cancer Center
John Asara
Beth Israel Deaconess Medical Center and Harvard Medical School
Florian Muller (fmuller@mdanderson.org)
Department of Cancer Systems Imaging, The University of Texas MD Anderson 8 Cancer Center, Houston, TX, 77054, USA https://orcid.org/0000-0001-7568-2948

Research

Keywords: Cancer Metabolism, Anaplerosis, Collateral Lethality, Glycolysis, Glutaminolysis, Enolase Inhibitor, POMHEX, CB-839

Posted Date: December 15th, 2020

DOI: https://doi.org/10.21203/rs.3.rs-125147/v1

Abstract

Reprogramming of metabolic pathways is crucial to satisfy the bioenergetic and biosynthetic demands and maintain the redox status of rapidly proliferating cancer cells. In tumors, the tricarboxylic acid (TCA) cycle generates biosynthetic intermediates by oxidation of anaplerotic substrates, such as glucose-derived pyruvate and glutamine20 derived glutamate. We have previously documented that a subset of tumors with 1p36 homozygous deletion exhibit co-deletion of ENO1, in turn becoming extremely dependent on its redundant isoform ENO2 and sensitive to an overall enzymatic deficiency of enolase. Metabolomic profiling of ENO1-deleted glioma cells treated with an enolase inhibitor revealed a profound decrease in TCA cycle metabolites, which correlated with cell-line specific sensitivity to enolase inhibition, highlighting the importance of glycolysis derived pyruvate for anaplerosis. Correspondingly, the toxicity of the enolase inhibitor was significantly attenuated by exogenous supplementation of supraphysiological levels of anaplerotic substrates including pyruvate. These findings led us to hypothesize that cancer cells with ENO1 homozygous deletions treated with an enolase inhibitor might show exceptional sensitivity to inhibition of glutaminolysis because of reduced anaplerotic flow from glycolysis. We found that ENO1-deleted cells indeed exhibited selective sensitivity to the glutaminase inhibitor CB-839, and this sensitivity was also attenuated by exogenous supplementation of anaplerotic substrates including pyruvate. Despite these promising in vitro results, the antineoplastic effects of CB-839 as a single agent in ENO1-deleted xenograft tumors in vivo were modest in both intracranial orthotopic tumors, where the limited efficacy could be attributed to the blood brain barrier (BBB), and subcutaneous xenografts, where BBB penetration is not an issue. This contrasts with the enolase inhibitor HEX, which, despite its negative charge, achieved antineoplastic effects in both intracranial and subcutaneous tumors. Together, these data suggest that at least for 1p36-deleted gliomas, tumors in vivo—unlike cells in culture—show limited dependence on glutaminolysis and instead primarily depend on glycolysis for anaplerosis. Our findings reinforce the previously reported metabolic idiosyncrasies of the in vitro and in vivo environments as the potential reasons for the differential efficacy of metabolism targeted therapies in in vitro and in vivo systems.

Full Text

This preprint is available for download as a PDF.

Tables

Due to technical limitations, table 1 is only available as a download in the Supplemental Files section.

Figures

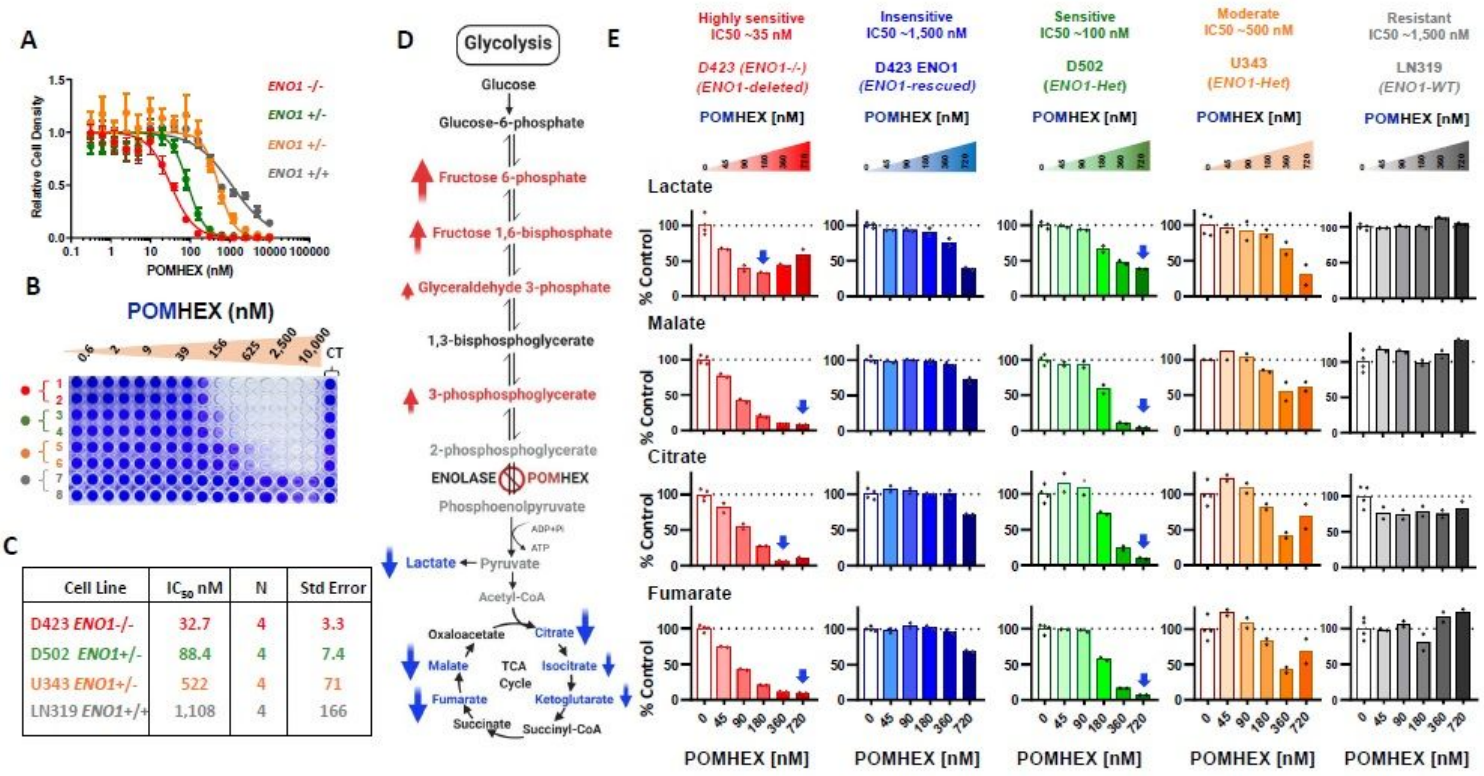

Cell Line	IC_{50} nM	N	Std Error
D423 *ENO1-/-*	32.7	4	3.3
D502 *ENO1+/-*	88.4	4	7.4
U343 *ENO1+/-*	522	4	71
LN319 *ENO1+/+*	1,108	4	166

Figure 1

Metabolomic profiling of Enolase inhibitor treated glioma cell lines indicates a profound disruption in anaplerosis, which correlates with the sensitivity A C Sensitivity of glioma cells to the enolase inhibitor is reflected by their ENO 1 status A Dose response curves of ENO 1 homozygously deleted (D 423 red, N= 4 ENO 1 heterozygously deleted (D 502 green, N= 4 U 343 orange, N= 4 and ENO 1 wild type (LN 319 grey N= 4 cells treated with the enolase inhibitor POMHEX at the indicated doses Error bars represent standard error of mean B After 5 days of treatment, the cells were fixed in 10 formalin and stained with crystal violet dye to measure the terminal cell density The terminal cell density is expressed relative to the untreated controls C A representative table with the IC 50 values of POMHEX across different cell lines strongly indicates that ENO 1 homozygously deleted cells are selectively sensitive, while ENO 1 heterozygotes display intermediate sensitivity to POMHEX D E Enolase inhibitor causes a profound disruption in the TCA cycle Cells were treated with varying concentrations of POMHEX in DMEM media and the metabolites were extracted in 80 cold methanol after 72 hours of drug treatment The extracted metabolites were subjected to metabolomic analysis by mass spectroscopy D Schematic showing the glycolytic and TCA cycle metabolites that are altered by POMHEX treatment E Lactate levels are shown as an indicator of glycolysis inhibition in response to the enolase inhibitor POMHEX Two TCA cycle intermediates citrate and malate are shown as representative metabolites in the TCA cycle that are altered in a dose dependent manner as a result of enolase inhibition The effects of enolase inhibition on TCA cycle metabolites correlate with the levels of ENO 1 in different cell lines, with the ENO 1 homozygously deleted cells exhibiting the most profound change, followed by ENO 1 heterozygous cells

showing intermediate effect while ENO 1 intact wild type cells sustaining no significant effect ..(See supplemental figure S 1 and S 2 a full panel of glycolytic and TCA cycle metabolites

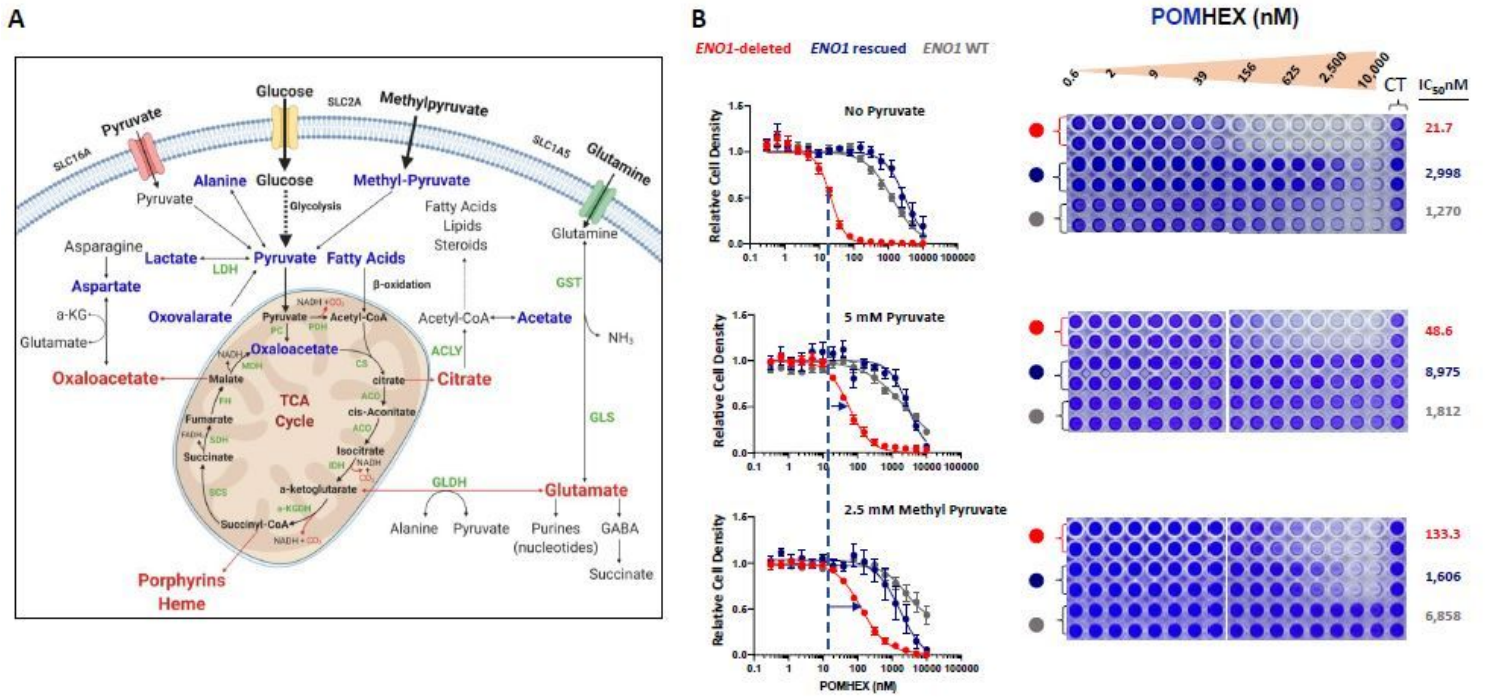

Figure 2

Exogenous supplementation of selected anaplerotic substrates mitigates the toxicity of enolase inhibition A Schematic representing different cellular metabolites that converge to replenish TCA cycle carbon atoms Exogenously supplemented anaplerotic substrates (acetate, aspartate, fatty acids, lactate, methylpyruvate pyruvate, oxaloacetate, and oxovalerate are indicated in blue, while cataplerotic substrates are indicated in red B Dose response curves of ENO 1 deleted, ENO 1 rescued and ENO 1 wild type cells to POMHEX in pyruvate free medium (12 and medium exogenously supplemented with 5 mM pyruvate (6 and 2 5 mM methyl pyruvate (4 Cells were seeded in 96 wells plates in pyruvate free DMEM or DMEM supplemented with anaplerotic substrates and treated with serial dilutions of POMHEX Crystal violet staining was performed to measure the terminal cell density and assess the effect of POMHEX and the degree of rescue of POMHEX toxicity by exogenous supplementation of anaplerotic substrates Cell density is expressed relative to the untreated controls A shift in IC 50 indicates alleviation of POMHEX toxicity by addition of exogenous anaplerotic substrates IC 50 of POMHEX for each cell line in different medium condition is indicated (See Supplemental Figure S 3 for a panel of anaplerotic substrates)

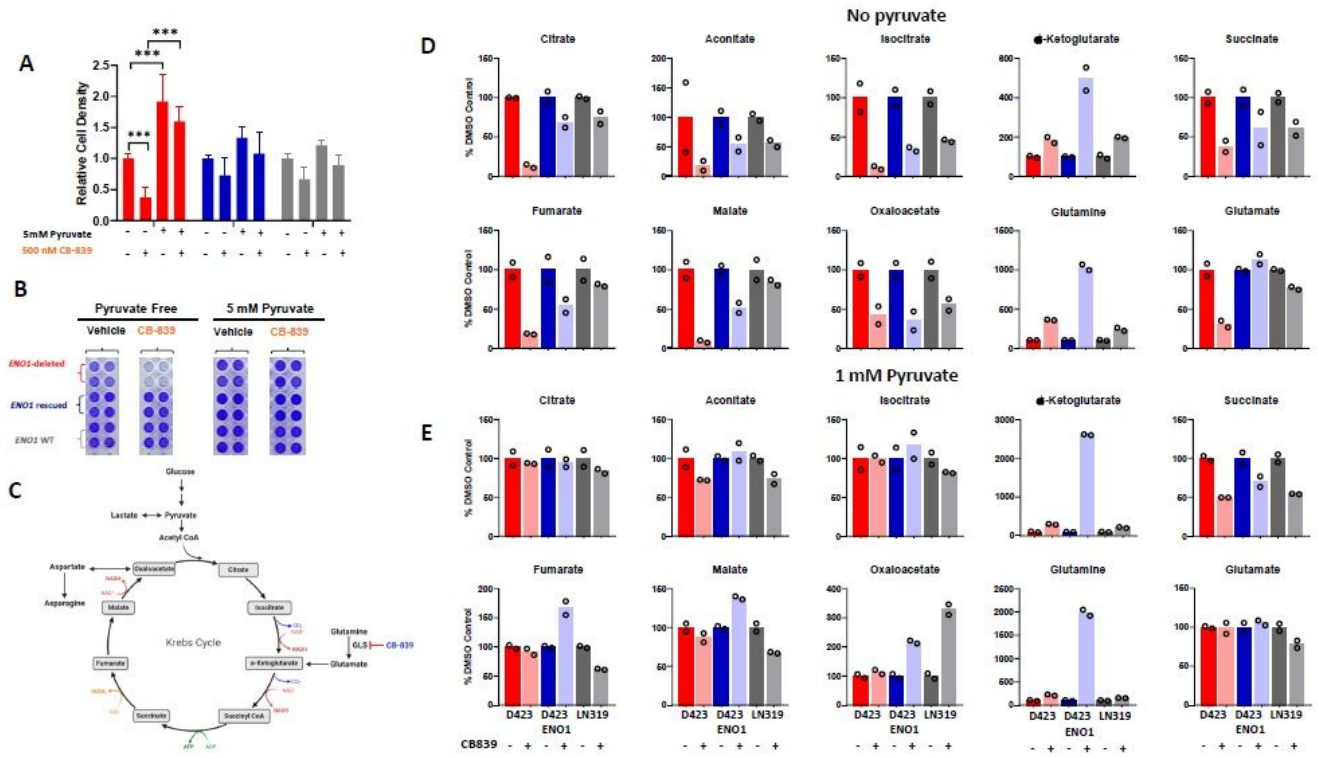

Figure 3

Media pyruvate availability modulates sensitivity to glutaminase inhibitor A Cells were treated with 500 nM CB 839 in either pyruvate free DMEM or DMEM supplemented with 5 mM pyruvate for 5 days Crystal violet staining was performed to determine the effect of CB 839 on cell growth Cell density is expressed relative to vehicle control in pyruvate free medium ENO 1 deleted N= 16 ENO 1 rescued N= 16 and ENO 1 WT N= 16 Mean and S D are shown Where indicated, represent statistical significance (0 0001 determined by 2 way ANOVA and Tukey's post hoc analysis B Metabolic map representing the intermediates in the central carbon metabolic pathways CB 839 targets glutaminase, the enzyme that converts glutamine to glutamate, and impedes glutamate anaplerosis to the TCA cycle C,D Metabolomics analysis reveal TCA cycle intermediate depletion as a major consequence of CB 839 treatment Cells were treated with 500 nM CB 839 in pyruvate free or regular DMEM 1 mM Pyruvate) for 72 hours and metabolites were extracted in 80 cold methanol and metabolite abundance was determined by MS Representative TCA cycle metabolites that are altered into CB 839 treatment in pyruvate free C and pyruvate replete DMEM D

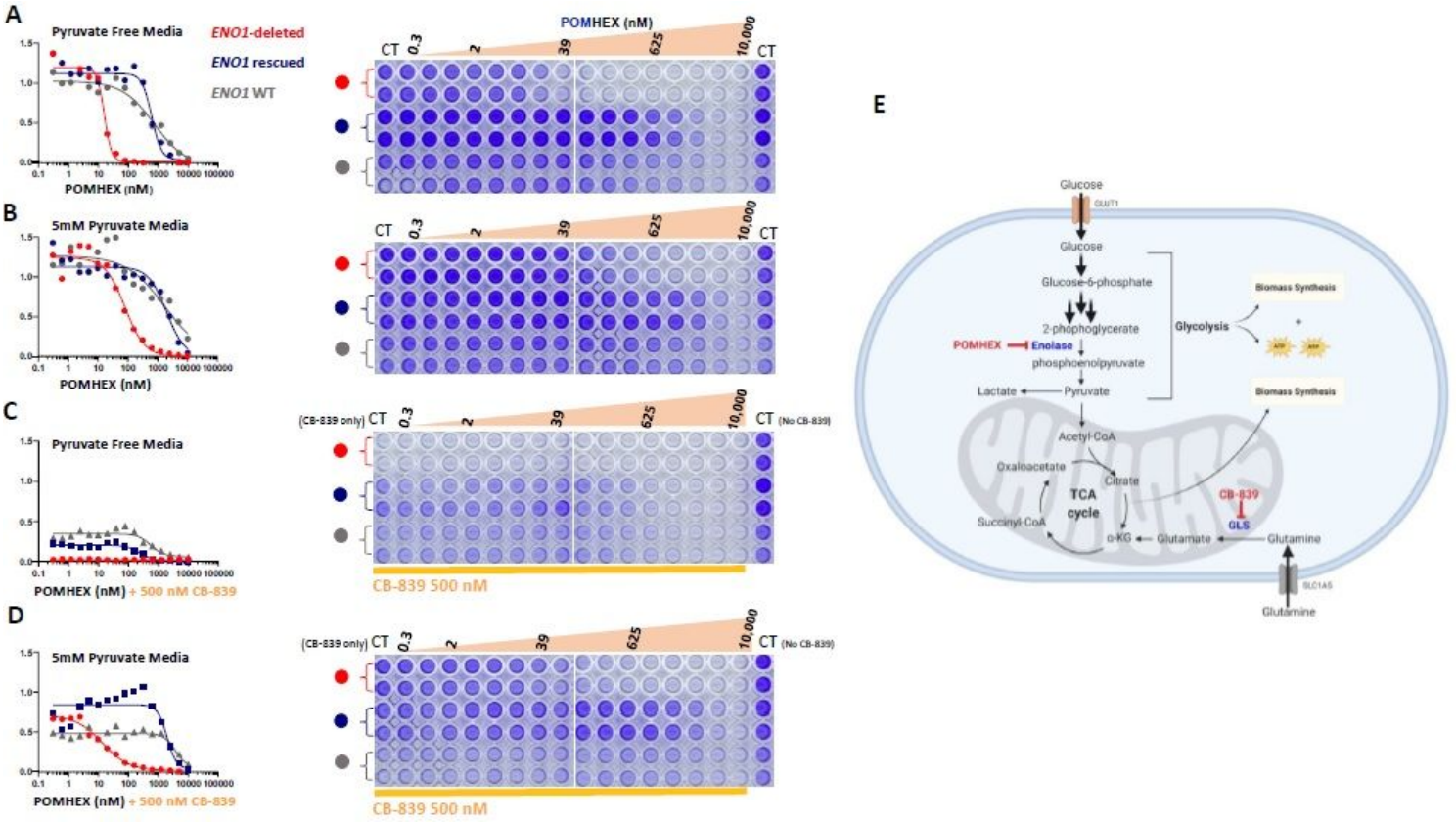

Figure 4

Synergistic anti neoplastic effect of POMHEX and CB 839 in pyruvate free condition ENO 1 homozygously deleted (D 423 red, N= 2 ENO 1 isogenically rescued (D 423 ENO 1 blue, N= 2 and ENO 1 WT (LN 319 grey, N= 2 cells were seeded in 96 well plates After 24 hours, the cells were treated with serial dilutions of POMHEX alone A and B or in combination with a fixed 500 nM CB 839 in pyruvate free and pyruvate supplemented medium Columns 1 2 vehicle control 3 10 serial dilutions of POMHEX and constant 500 nM CB 839 11 12 constant 500 nM CB 839 C and D The cells were grown in pyruvate free A and C or 5 mM pyruvate supplemented medium B and D Following 5 days of drug treatment, cells were fixed and crystal violet staining was performed to determine cell density in response to the drug treatment Data are expressed relative to the untreated control Note the substantial synergy between POMHEX and CB 839 which is accentuated in pyruvate free condition C and partially reversed by pyruvate supplementation D E Schematic showing the inhibition of glycolysis by POMHEX at the enolase step, and inhibition of glutaminolysis by CB 839 both converging to impede TCA cycle anaplerosis at different steps of the cycle Combined inhibition of glycolysis and glutaminolysis especially under pyruvate free conditions could synergistically deplete TCA cycle intermediates and induce dramatic cell death

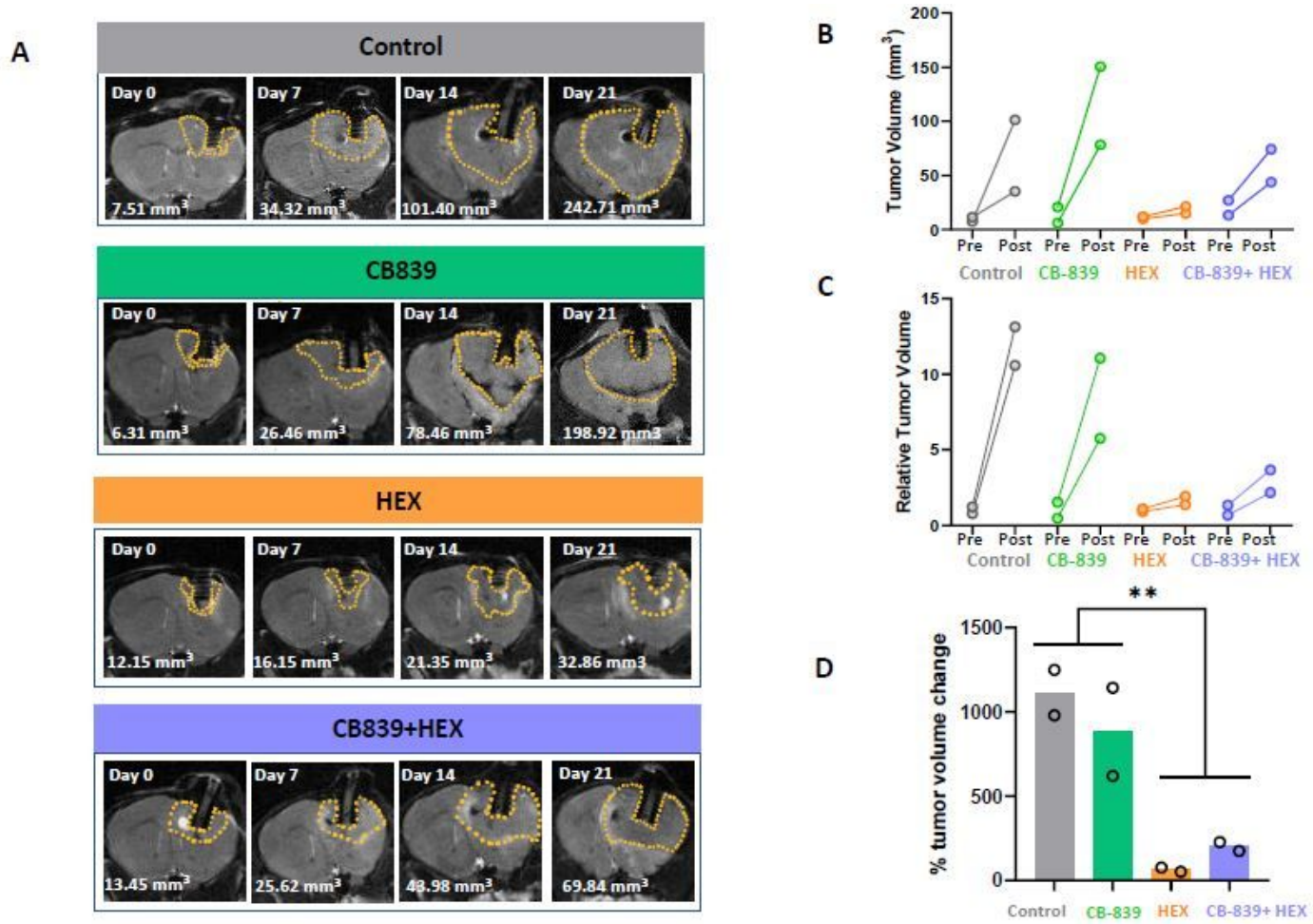

Figure 5

CB 839 and HEX combination attenuates intracranial tumor growth but does not cause a frank tumor regression ENO 1 deleted glioma cells (D 423 were implanted intracranially in immunocompromised nude mice and tumor growth was monitored weekly by T 2 MRI Tumors are MRI detectable (indicated by dashed yellow outlines) 20 30 days after tumor implantation 3 D Slicer was used to view the DICOM files and measure tumor volumes A Representative MRI images to indicate weekly changes in tumor volume across different treatment groups, Control (2 CB 839 treated 200 mpk BID orally N= 2 HEX treated 300 mpk SC N= 2 CB 839 +HEX 200 mpk CB 839 BID orally, and 300 mpk HEX SC N= 2 Following the completion of treatment course, animals were sacrificed, and the brains were dissected and fixed in formaldehyde for histopathological analyses B Pre and post treatment comparison of absolute and relative tumor volumes across different treatment groups C Percent change in tumor volume after two weeks of drug treatment

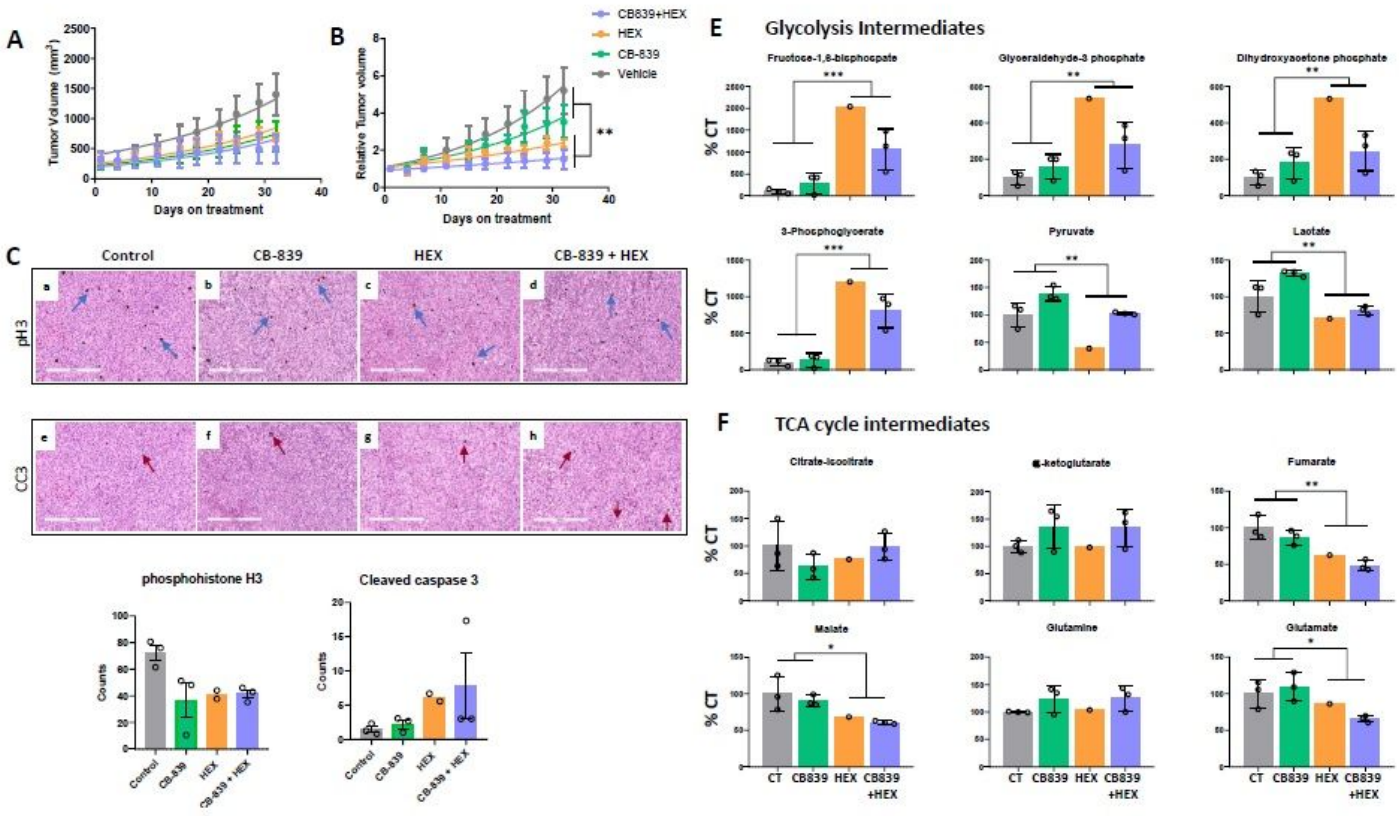

Figure 6

Glutaminase inhibition does not show anti tumor activity against ENO1 deleted subcutaneous tumors. ENO 1 deleted glioma cells (D 423 were implanted subcutaneously in immunocompromised nude mice and once the tumors reached 200 mm 3 mice were randomly assigned into different treatment groups Vehicle control (3 CB 839 200 mpk BID orally N= 3 HEX 300 mpk SC N= 3 CB 839 +HEX 200 mpk CB 839 BID orally, and 300 mpk HEX SC N= 3 A B Tumor volume changes in response to the drug treatment was determined by measuring tumors three times a week using Vernier's calipers A Absolute tumor volume (mm 3 and B Relative tumor volume growth curves during one month treatment course Following the completion of treatment course, animals were sacrificed, and the tumors were dissected and fixed in formalin for histopathological analyses or frozen in liquid nitrogen for metabolomic analyses C D IHC staining for cell proliferation marker (phospho histone 3 ,pH 3 black stain, blue arrows) and marker of apoptosis (cleaved caspase 3 CC 3 black stain, red arrows) in tissue sections of control, CB 839 HEX and CB 839 HEX treated tumors size bar, 300 µm D Counts of p H 3 and CC 3 positive cells per 100 X section are shown E F Metabolomic analysis of frozen tumors show key differences in metabolites upstream and downstream of enolase reaction in HEX treated tumors Tumors were extracted approximately 4 6 hours after the final dose Representative glycolytic intermediates (top panel, E and TCA cycle intermediates (bottom panel, F altered in response to drug treatments Metabolites are expressed relative to the vehicle control ..(N= 3 CB 839 N= 3 HEX, N= 1 and CB 839 HEX, N= 3 Mean and S D where relevant with individual data points are shown) Where indicated, represents statistical significance (0 05 achieved by 2

way ANOVA and Tukey's post hoc analysis ..(Metabolomics data represented in this panel were obtained using metabolomics core at BIDMC and included N= 1 HEX treated tumor Remaining HEX treated tumors from this experiment were used for metabolomics with the Metabolon Inc platform See supplemental Figure S 7

Supplementary Files

This is a list of supplementary files associated with this preprint. Click to download.

- SupplmentaryFigures1and2.pdf
- SupplementalFigures.pdf
- Table1.JPG